Hindawi
Mathematical Problems in Engineering
Volume 2021, Article ID 7246488, 12 pages
https://doi.org/10.1155/2021/7246488

Research Article

Time-Frequency Characteristics of Fluctuating Pressure on the Bottom of the Stilling Basin with Step-Down Floor Based on Hilbert–Huang Transform

Wang Jia, Mingjun Diao, Lei Jiang, and Guibing Huang

State Key Laboratory of Hydraulics and Mountain River Development and Protection, Sichuan University, 24 South First Ring Road, Wuhou District, Chengdu 610065, China

Correspondence should be addressed to Mingjun Diao; diaomingjun@scu.edu.cn

Received 20 July 2021; Revised 10 August 2021; Accepted 16 August 2021; Published 7 September 2021

Academic Editor: Francesco Aristodemo

Fluctuating pressure is an important feature of the bottom of a stilling basin with step-down floor. To analyze the frequency domain characteristics and energy distribution of this fluctuating pressure, the Hilbert–Huang transform (HHT) method is used. First, empirical mode decomposition is performed on the pressure fluctuation signal to obtain a number of intrinsic mode functions (IMFs), and then the Hilbert transformation is performed on each IMF to obtain the Hilbert spectrum and marginal spectrum for characterizing the pressure fluctuation signal. The results show that the fluctuating pressure signal of the stilling basin with step-down floor has obvious characteristics of low frequency and large amplitude. The dominant frequencies of the head and tail of the stilling basin are very prominent, and most of the energy is concentrated below 5.0 Hz; with the increase in the relative position of the measuring point, the energy distribution in stilling basin with step-down floor changes from high-frequency component to low-frequency component. The fluctuating pressure signal of the stilling basin with step-down floor has random amplitude modulation and frequency modulation. The marginal spectrum obtained by the HHT method can obtain the local characteristics of the signal more accurately and is more suitable for processing nonlinear and nonstationary signals.

1. Introduction

In recent years, with the continuous increase in the number of high dam water conservancy projects, research on energy dissipation and antiscouring technology under high water head and high flow conditions has become increasingly important [1]. To this end, researchers have proposed a series of new energy dissipation structures to meet the energy dissipation requirements under such extreme conditions. Stilling basin with step-down floor is a representative new energy dissipation structure [2]. Figure 1 shows a schematic diagram of a conventional stilling basin and a stilling basin with step-down floor. The stilling basin with step-down floor has a sill at the head of the conventional stilling basin to improve the hydraulic properties of the stilling basin floor. When the water flow is injected into the stilling basin, the main flow does not submerge below the surface or form a surface flow. On the one hand, this approach reduces the impact pressure on the bottom of the stilling basin; on the other hand, it reduces the impact on downstream navigation. In addition, compared with conventional stilling basins, the sloping underflow stilling basin can not only ensure a higher energy dissipation rate but also significantly reduce the erosion of the bottom plate in the stilling basin [3]. Because of its many advantages, an increasing number of high dam projects have adopted this form of energy dissipation.

For a conventional stilling basin or a stilling basin with step-down floor, the fluctuating pressure on the bottom of the basin is an important cause of erosion damage [4]. The violent pulsation of hydrodynamic pressure on the bottom of the stilling basin results in an increase in the instantaneous load acting on the bottom, which increases the possibility of vibration and cavitation of the bottom. In

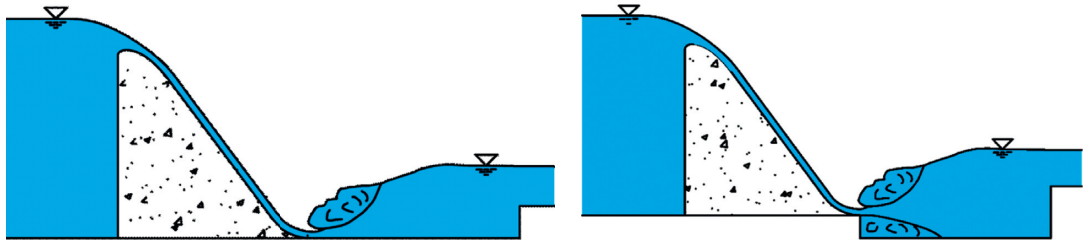

(a) (b)

Figure 1: Structure diagram of stilling basin: (a) conventional stilling basin; (b) stilling basin with step-down floor.

engineering practice, it is not uncommon for the fluctuating pressure to cause instantaneous instability and destruction of the bottom plate of a stilling basin [5], such as the serious damage to the stilling basin bottom plate of the Sayan hydropower station in the former Soviet Union and the anchor bars of the bottom floor of the stilling basin that were broken or pulled during the operation of the Malpaso Project in Mexico. Therefore, studying the fluctuating pressure characteristics of a stilling basin with step-down floor is very significant for engineering practice.

To understand the basic characteristics of the fluctuating pressure at the bottom plate of a stilling basin with step-down floor, many scholars have carried out related research. In existing research, the mathematical statistics method and the power spectrum analysis approach are the two most commonly used methods for studying the characteristics of the fluctuating pressure in a stilling basin with step-down floor.

Thus, Lu et al. [6] studied the pulsating pressure distribution of the bottom of the stilling pool and provided a research method that combines the quantitative analysis of pulsating velocity, pulsating vortex, and other influencing factors with the qualitative analysis of pulsating vortex. Armenio et al. [7] studied the turbulent pressure fluctuations at the bottom of the stilling basin with step-down floor, focusing on the analysis of the extreme value of the pulsating pressure anisotropy field and the spatial correlation structure; Kazemi et al. [8] studied the distribution of fluctuating pressure and the location of the most severe fluctuating pressure through the physical model. Yang et al. [9] conducted a comprehensive analysis of the distribution law and time-frequency characteristics of the pulsating pressure on the floor of the slam still basin through model tests. Mathematical statistics and spectrum analysis methods are helpful to further understand the characteristics of the fluctuating pressure. However, stilling basin on step-down floor fluctuating pressure signal has certain nonstationary characteristics and insufficient to study it only in the time domain. Traditional Fourier transform analysis can transform the entire signal from the time domain to the frequency domain for analysis, but a disadvantage of this approach is that it cannot reflect the instantaneous frequency change in the signal. Later, some scholars adopted the windowed Fourier transform technique to obtain the time-frequency characteristics of the fluctuating pressure. However, this method also has certain drawbacks. For example, once the window function is selected, it cannot be modified arbitrarily, and the influence of the window function on the result is difficult to estimate.

In 1998, Huang et al. a Chinese-American scientist proposed a new signal processing method called the Hilbert–Huang transform (HHT) [10]. The HHT method first decomposes the signal into several intrinsic mode functions (IMFs) through empirical mode decomposition (EMD) and then performs a Hilbert transform on each IMF component to obtain the instantaneous frequency and instantaneous amplitude of each IMF, thereby constructing the output of the time-frequency energy distribution of the signal, that is, the Hilbert spectrum. The decomposition basis of the HHT method depends on the signal itself, so it has good adaptability, and because the method is decomposed with EMD, it also has the physical meaning of the EMD method and high time-frequency resolution [11]. Compared with the Fourier transform and wavelet transform, the HHT method can decompose the signal according to the inherent characteristics of the signal without artificially setting the basis function, and its high efficiency and adaptability are very suitable for processing nonlinear and nonstationary signals. Table 1 shows the advantages and disadvantages of fast Fourier transform, wavelet transform, and Hilbert–Huang transform.

It can be seen from the table that the HHT method does not need the stability and nonlinearity of the original signal and does not need to set the basis function in advance [12]. The marginal spectrum reflects the actual change of the signal more accurately. In dealing with nonstationary and nonlinear data, Hilbert–Huang transform is more suitable than fast Fourier transform and wavelet transform [13]. Therefore, the HHT method is widely used in various fields.

In the biomedical field, the HHT method is often used for signal feature extraction. Especially in recent years, researchers have verified the effectiveness of this method when studying the time-frequency characteristics of human brain activity signals [14]. Thus, Kumar et al. [15] used the HHT method to recognize the power quality event and made it an attractive tool for analysis of power quality events; Hemapriya et al. [16] used Hilbert–Huang transform (HHT) to detect and identify complex power quality signals in smart grid power systems. This document analyzes the IMF components in detail and extracts the information of the original signal carried in the Hilbert spectrum. As a processing technique for nonstationary signals, the HHT

Table 1: Common signal processing methods.

Method	Merit	Defect
Fast Fourier transform	Complete theory and mature method	(1) Unable to extract local features from data (2) Not suitable for nonlinear and nonstationary data (3) Predetermined basis function (4) Fourier spectrum can only approximately reflect the actual situation
Wavelet transform	(1) Complete theory; methods mature (2) Nonstationary signals can be processed (3) Simultaneous energy-time-frequency information (4) Interwave frequency modulation can be given	(1) Not suitable for nonlinear data (2) Need to define base functions in advance (3) Intrawave frequency modulation cannot be given
Hilbert–Huang transform	(1) No requirements for data stability and nonlinearity (2) EMD decomposition does not require presupposition basis function (3) Simultaneous energy-time-frequency information (4) Instantaneous frequency has physical meaning and can reflect local characteristics of signal more accurately (5) Marginal spectra accurately reflect the actual situation	Incomplete theory belongs to empirical method

method can decompose the fluctuations or trends at different scales in the signal step by step and can describe the degree of nonstationarity of the signal. It can quickly and effectively capture signal transient characteristics and is very suitable for use in signal recognition, signal detection, and signal decomposition. The HHT method has played an enormous role in signal processing such as power systems biomedical and high-voltage transmission line protection. The abundant information contained in the fluctuating pressure signal of the stilling basin with step-down floor is of great value for theoretical research and engineering applications in stilling basin with step-down floor. It is necessary to study how the signal spectrum changes with time.

Therefore, this research attempts to use the HHT method to analyze the fluctuating pressure signal and to study the fluctuating pressure signal on the bottom plate of a stilling basin with step-down floor from a perspective that is different from the traditional one. First, EMD is used to extract the pressure measurement points, the IMF weight. Subsequently, using the Hilbert transform, the instantaneous amplitude and frequency of the IMF components at each measurement point were determined, and the time-frequency distribution and amplitude distribution of the fluctuating pressure signal were obtained. Based on the above results, the main frequency characteristics, time-frequency characteristics, and energy change laws of the fluctuating pressure of the stilling basin with step-down floor are analyzed. Finally, by comparing and analyzing the consistency of the spectrum analysis results with the flow pattern and the fluctuating pressure coefficient distribution law, the applicability of the HHT method in analyzing the fluctuating pressure signal of the stilling basin with step-down floor is proven.

2. General Model Test Setup

The physical model test system is composed of water supply system, rectangular weir, upstream reservoir, drainage channel, WES weir, and stilling pool. The model is made of organic glass. The length of the stilling pool is 2 m, the width is 0.5 m, the height of the tail sill is 0.2625 m, the height of the falling sill is 0.1 m, and the incident angle is 10°. The straight line segment is a steep slope drainage chute with a rectangular section with a slope of 53°. The schematic diagram of the model and the photo of the model are shown in Figure 2.

In order to study the characteristics of the water flow in the stilling basin of the falling sill under different working conditions, this paper designed four different flow experimental conditions: 30 m^3/s, 50 m^3/s, 70 m^3/s, and 90 m^3/s. The flow of the model is controlled by a rectangular thin-walled weir with an accuracy of 0.1 mm. Table 2 shows the four experimental conditions of the model test.

In order to describe the position of the pressure measurement point, a one-dimensional coordinate system with the central axis of the bottom of the stilling pool as the x-axis is established, and the coordinate origin is set at the intersection of the front end of the bottom of the stilling pool and the central axis. A total of 8 measuring points are arranged along the central axis of the stilling pool. The orifice diameter of the pressure measuring point is 2.0 mm. The relative position η of the measuring point is $\eta = x/\mathrm{L}$, where L is the length of the stilling pool, and the unit is m. Table 3 shows the relative position of each measuring point.

This article uses the SDA1000 high-performance digital sensor system to collect and process the pulsating pressure. In order to measure the pulsating pressure of the eight characteristic points on the bottom of the stilling pool at the same time, this experiment connects eight sensors to the hub and then connects the hub to the computer. The sampling frequency is $f = 100$ Hz, the sampling time is $t = 240$ s, and the total number of samples is $N = 24000$.

2.1. Basic Principles and Characteristics of the HHT. The basic idea of the HHT is to first decompose the signal into several intrinsic mode functions through EMD and then perform Hilbert transformation on each intrinsic mode function to

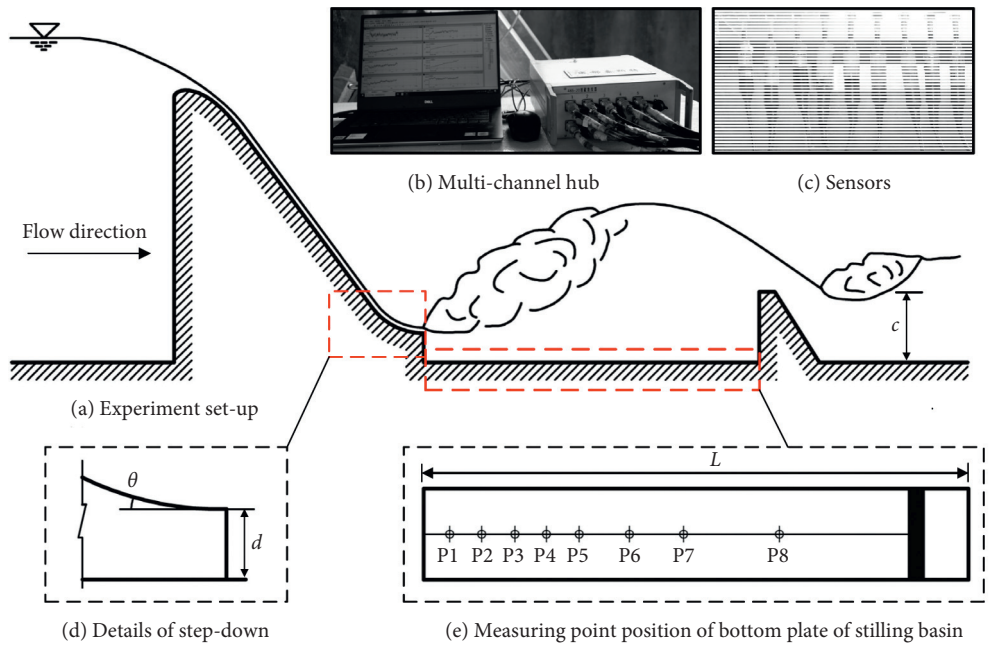

FIGURE 2: Model experiment setup: (a) the schematic diagram of the model; (b) the hub connected to the computer; (c) the sensor inserted on the bottom of the stilling pool; (d) the height of the slam and the angle of incidence; (e) the positional relationship of the measuring points on the bottom of the stilling pool.

obtain instantaneous frequency data [17]. The instantaneous frequency and instantaneous amplitude data of the signal are used to construct the time-frequency energy distribution of the signal, namely, the Hilbert spectrum [18]. The implementation steps of the HHT method are shown in Figure 3.

Taking time series data X_t as an example, the empirical mode decomposition algorithm is expressed as follows:

$$X(t) = \sum_{k=1}^{n} c_k(t) + r_n(t), \tag{1}$$

where $c_k(t)$ is the IMF component and $r_n(t)$ is the residual function, which represents the average trend of the signal.

Each IMF component contains components of different scales and scales from small to large [17]. Therefore, each component contains components from the high-frequency band to the low-frequency band, and each frequency band contains different frequency components, which vary with the signal itself [18].

The Hilbert transform is used to perform spectrum analysis on each IMF component to obtain the Hilbert time spectrum, referred to as the Hilbert spectrum, denoted as follows [17]:

$$H(\omega, t) = \mathrm{Re} \sum_{i=1}^{n} a_i(t) e^{j \int \omega_1(t) \mathrm{d}t}. \tag{2}$$

The Hilbert marginal spectrum is obtained by the time integral of the Hilbert spectrum as follows:

$$h(\omega) = \int_0^T H(\omega, t) \mathrm{d}t. \tag{3}$$

2.2. Pulse Pressure Signal Processing. In the model test, the pulsating pressure signals at eight characteristic points on the stilling basin with step-down floor were measured under four flow rates, and the sampling time of the pulsating pressure sensor was 240 s. In the model test, due to the existence of various noises, the fluctuating pressure signal of the stilling basin floor often produces distortion, so it is necessary to use a signal processing method to restore the true signal of fluctuating pressure. In this paper, the least square method and five-point cubic smoothing method are used to reprocess the fluctuating pressure signal of the stilling basin with step-down floor.

First, the IMF component is obtained through empirical mode decomposition. This section uses EMD to gradually decompose the fluctuations or trends of different scales in the signal. Each sequence is called an IMF. The decomposed IMF components accurately reflect the fluctuating pressure signal and the inherent characteristics [19]. When $Q = 90\ \mathrm{m^3/s}$ is selected, the fluctuating pressure signal at the measuring point $\eta = 0.025$ is subjected to EMD. Nine IMF components and 1 residual term are obtained through EMD. The nine IMF components and its corresponding Fourier spectrum are shown in Figure 4.

Figure 4 shows that the original signal is decomposed into 10 IMF components. The decomposition process does not need to rely on any basis functions. The IMF components are decomposed according to the characteristics of the original signal. Therefore, this article considers the EMD decomposition process to be an adaptive process. It can be seen from Figure 4 that IMF1 has the widest frequency band. According to the order of decomposition, the frequency band of the decomposed IMF components gradually narrows. IMF1 and IMF2 are the high-frequency bands of the

Table 2: Table of experimental conditions.

Test plan	Q (m³/s)	q	H (m)
a	30	0.06	131.12
b	50	0.10	134.40
c	70	0.14	136.88
d	90	0.18	139.20

Table 3: The measuring point position table on the central axis of the bottom plate of the stilling pool.

Measuring point number	η
P1	0.025
P2	0.075
P3	0.125
P4	0.175
P5	0.225
P6	0.325
P7	0.45
P8	0.64

signal, showing the characteristics of high frequency and fast attenuation, and the energy is mainly concentrated on these two components; IMF3, IMF4, and IMF5 are between 1 and 5.0 Hz; IMF6 ~ IMF10 are low-frequency bands, which contain very little energy.

The IMF components are decomposed from large to small time scales, and the frequency of the IMF components decreases with the decomposition. The IMF components decomposed by EMD have practical physical meaning and can reflect the local characteristics of the signal more accurately. There may be components with the same time scale and frequency in each IMF component, but they do not appear at the same local location of each component, suggesting that each IMF component truly reflects any local oscillation in the original signal [18].

Next, we apply Hilbert–Huang transform to the decomposed IMF components to obtain the Hilbert–Huang spectra of each component. When $Q = 90$ m³/s, the fluctuating pressure signal at $\eta = 0.025$ on the central axis of the stilling basin with a drop sill is decomposed by EMD to obtain 10 IMF components. Each IMF component is subjected to the Hilbert transform to obtain its energy-frequency-time Hilbert–Huang spectrum [17]. This paper uses IE to represent the energy value of the Hilbert–Huang spectrum of IMF components. Since the energy contained in the final IMF component is very small, Figure 5 shows the Hilbert spectrum of the first 6 IMF components, which describes the local change characteristics of the signal in the time domain and frequency domain.

As shown in Figure 5, the Hilbert spectrum of each IMF component shows the variation of energy with frequency and time and can also reflect the corresponding instantaneous frequency and time when the energy reaches its peak. The energy of IMF1 is concentrated in 0~15 Hz, the energy of IMF2 is concentrated in 0~10 Hz, the energy of IMF3 is concentrated in 0~5 Hz, and the energy of IMF4 is concentrated in 0~3 Hz. According to the decomposition order, the Hilbert energy gradually decreases and the frequency band gradually narrows, indicating that the EMD decomposition gradually separates the signal components from high to low frequencies; the instantaneous energy and instantaneous frequency of IMF components change with time, indicating that each IMF component has the form of frequency and amplitude modulation; the frequency of each IMF component changes with time, and the change of its waveform means that the frequency modulation within the wave occurs; the frequency difference of different IMF components indicates the modulation between waves, and the fluctuating pressure signal is a complex signal with both interwave frequency modulation and intrawave frequency modulation, which is due to the impact of the drained water on the stilling basin floor, the vortex rotation speed inside the water is very fast, and the lateral movement of the fluid particle is very strong, so that the flow is highly turbulent, and the fluctuating hydrodynamic pressure is very intense. The Hilbert–Huang transform shows the nonlinear and nonstationary properties of pressure pulsation [20], and it truly reveals that the pressure pulsation signal has nonlinear random modulation and impact properties [21].

Next, this article integrates the results of the Hilber–tHuang transform with respect to time to obtain the Hilbert marginal spectrum. The Hilbert marginal spectrum has a certain probability meaning. The existence of energy at a certain frequency indicates that the vibration of that frequency may occur. Then, the frequency corresponding to the maximum value of the marginal spectrum amplitude is the most likely vibration frequency, which is the dominant frequency that this article is most concerned about. This article will use the Hilbert marginal spectrum to study the energy transfer law of pulsating pressure signals. Figure 6 shows the Hilbert marginal spectrum of the characteristic points on the bottom of the stilling pool under different flow rates. Tables 4 and 5 are the dominant frequency table and the marginal spectrum amplitude table of the different characteristic points on the central axis of the bottom of the stilling pool.

Figure 3: Signal processing flow chart using the HHT method.

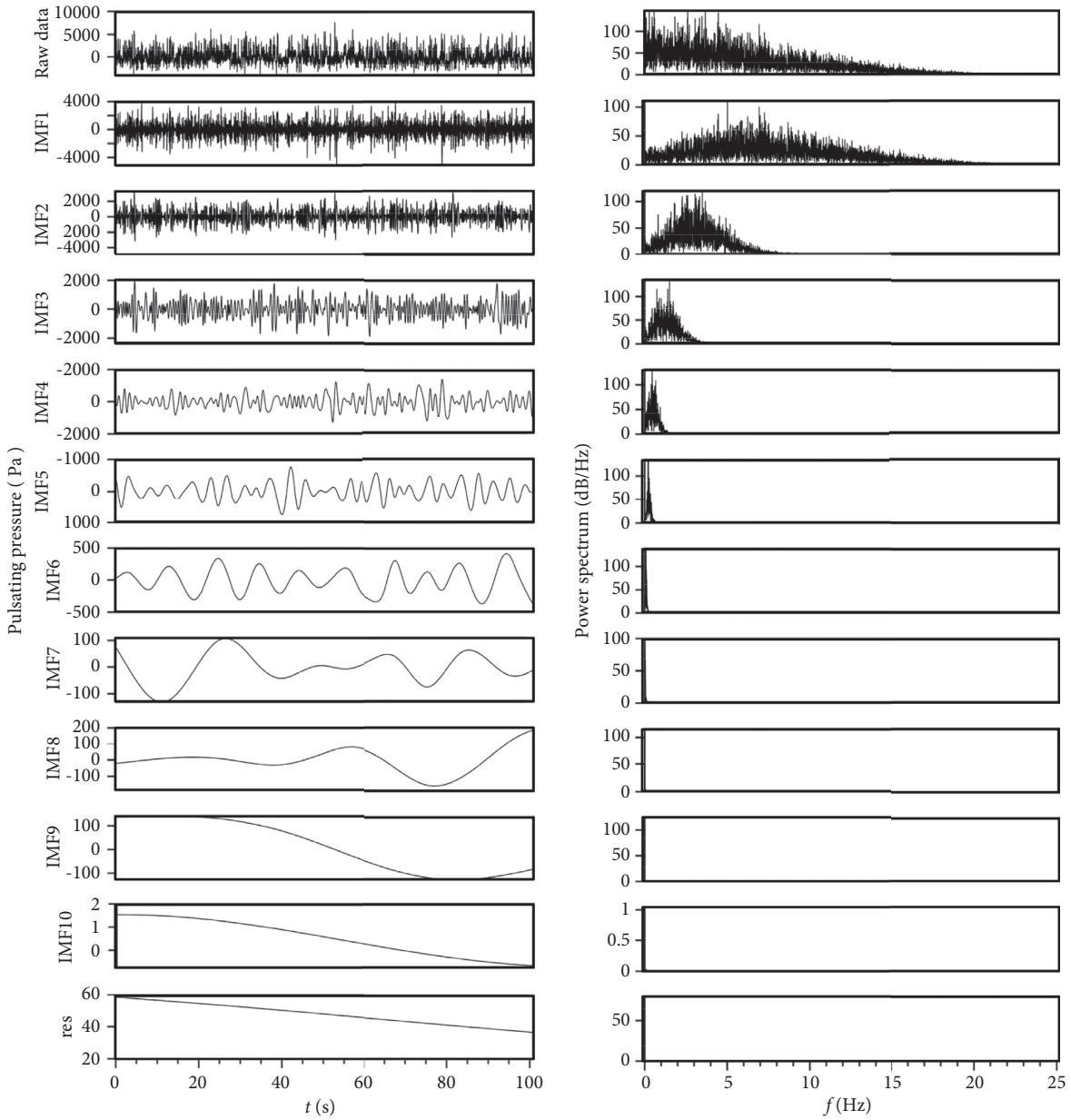

Figure 4: The IMF components and its Fourier spectrum.

It can be seen from Figure 6 and Tables 4 and 5 that when $Q = 30\ m^3/s$, at $\eta = 0.025$, the dominant frequency is 5.0 Hz, and the marginal spectrum amplitude is 9.2×10^4; at $\eta = 0.075$, the dominant frequency is 3.6 Hz, and the marginal spectrum amplitude is 10.3×10^4Pa; the dominant frequencies of the other positions are less than 5.0 Hz. When $Q = 50\ m^3/s$, at $\eta = 0.075$, the marginal spectral amplitude reaches the peak value of 4.19×10^6Pa, the marginal spectral amplitude decreases gradually after the peak point, and the dominant frequency at all feature points is less than 5.0 Hz. When $Q = 70\ m^3/s$, at $\eta = 0.075$, the marginal spectral amplitude reaches the peak value of 1.2×10^7Pa, the marginal spectral amplitude decreases gradually after the peak point, and the dominant frequency at all feature points is less than 5.0 Hz. When $Q = 90\ m^3/s$, at $\eta = 0.075$, the amplitude reaches the peak value of 2.04×10^7Pa. After the peak point, the

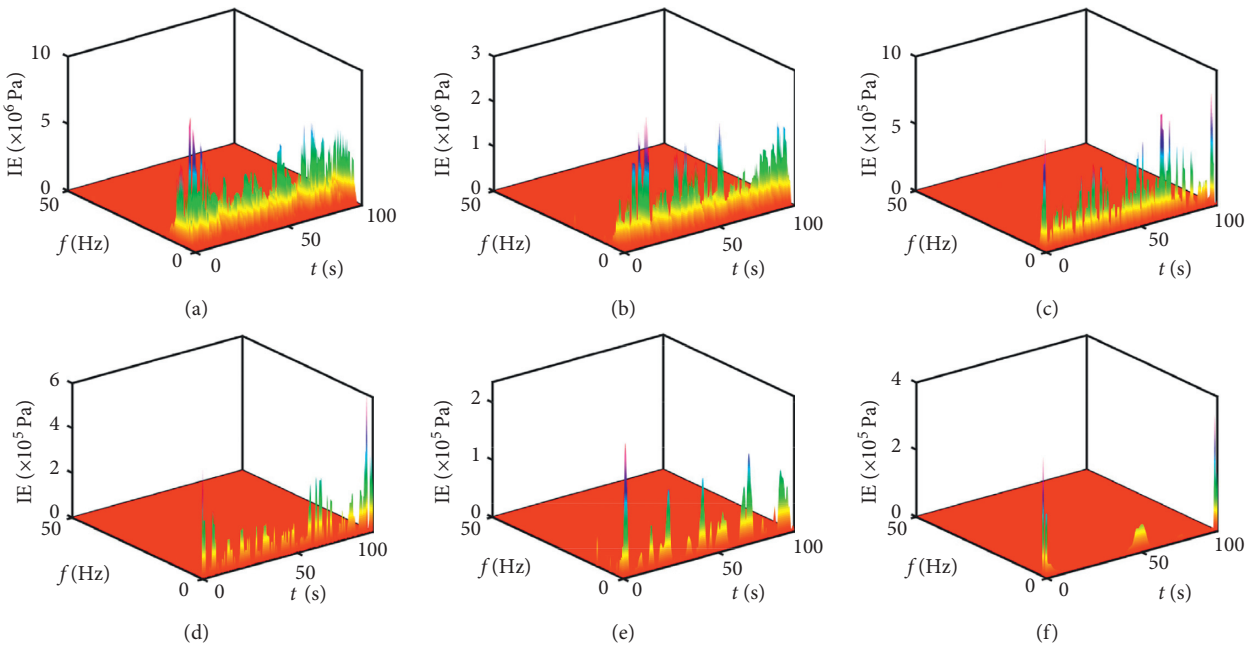

Figure 5: Hilbert spectra of the first 6 IMF components.

marginal spectrum amplitude gradually decreases, and the dominant frequency at all feature points is less than or equal to 5.0 Hz.

In summary, the dominant frequencies of the characteristic points of the stilling basin floor are not more than 5.0 Hz, and the fluctuating pressure distribution has obvious low-frequency characteristics. The fluctuating energy in the swirling region of water flow in front of stilling basin is mainly distributed within 0~5.0 Hz. The water flow in the back of the stilling basin is relatively stable, and the fluctuating energy is mainly distributed within 0~2.5 Hz. The dominant frequency in the front of stilling basin is greater than that in the middle and back. It indicates that stilling basin has a good energy dissipation effect; the amplitude of the marginal spectrum at $\eta = 0.075$ is much larger than that at other positions, indicating that the jet impingement point on the stilling basin floor is located near $\eta = 0.075$. The water flow in the impingement zone is highly turbulent, and the pressure fluctuation is very intense. Near the jet impingement point, the signal energy is mainly concentrated in the low-frequency region; that is, the energy is mainly concentrated in the large-scale fluid vortex [22].

3. Discussion

3.1. Energy Conversion of IMF Components. This paper divides the IMF obtained by EMD into three frequency bands: low-frequency band (less than 1 Hz), midfrequency band (1 to 5 Hz), and high-frequency band (above 5 Hz). To facilitate the analysis of the law of the energy change with the relative position, the energy of each IMF order of the fluctuating pressure signal is calculated, that is, the mean square value; in addition, the percentage of energy in the high-, middle-, and low-frequency bands is obtained, giving a curve with respect to the relative position change. In this paper, ER is used to represent the proportion of energy. Figure 7 shows the trend of low-, medium-, and high-frequency energy under different flow rates.

It can be seen from Figure 7 that when $Q = 30\ m^3/s$, $Q = 50\ m^3/s$, $Q = 70\ m^3/s$, and $Q = 90\ m^3/s$, the proportion of high-frequency energy decreases with the increase in the relative position η of the measuring point. The proportion of medium-frequency energy and low-frequency energy increases gradually. The distribution of energy changes from low-order IMF component to high-order IMF components. The high-frequency components are dominant, and the low-frequency component is dominant. The conversion process of this energy distribution is mainly caused by the low-frequency modulation of fluid particle motion. According to the basic theory of turbulence, the high-frequency band mainly exists in the fluid vortex with small scale, and the low-frequency band mainly exists in the fluid vortex with large scale. The energy of the fluctuating pressure signal changes from high-frequency dominant to low-frequency dominant, which means that the small-scale vortex in the stilling basin with step-down floor changes into large-scale vortex [23]. The Hilbert–Huang transform directly reveals the inherent law that the energy distribution of IMF component of EMD decomposition of the pressure pulsation signal changes with the relative position of the measuring point [24].

3.2. Fourier Spectrum and Marginal Spectrum. First, the fast Fourier transform is used to analyze the pulsating pressure, and the power spectral density of the pulsating pressure is calculated. Figure 8 shows the TX15 stilling pool. Figure 8 shows the power spectrum density and marginal spectrum of

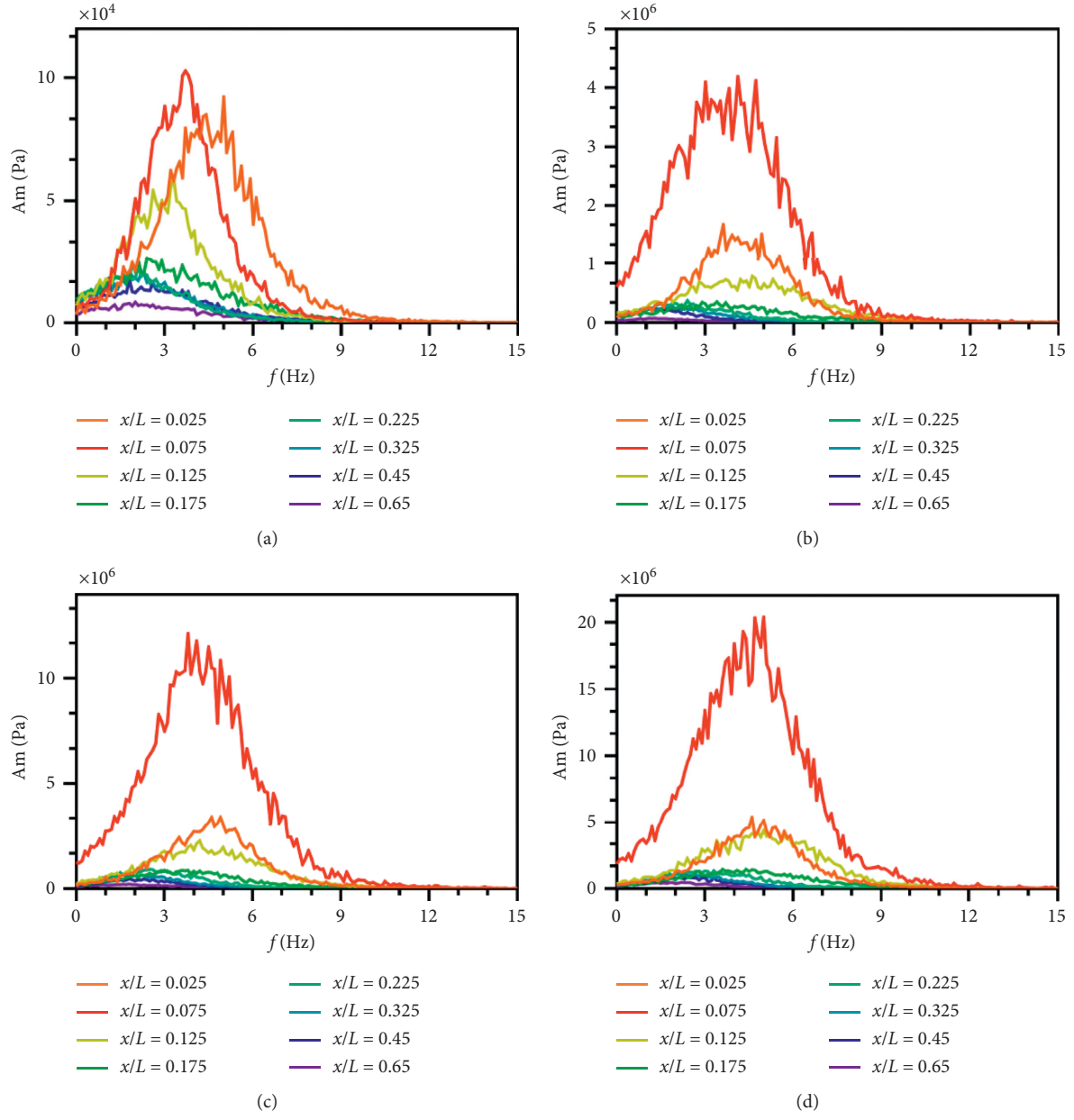

Figure 6: Marginal spectra of characteristic points: (a) $Q = 30\ m^3/s$; (b) $Q = 50\ m^3/s$; (c) $Q = 70\ m^3/s$; (d) $Q = 90\ m^3/s$.

Table 4: Frequency advantage table (Hz).

Q (m^3/s)	$\eta = 0.025$	$\eta = 0.075$	$\eta = 0.125$	$\eta = 0.175$	$\eta = 0.225$	$\eta = 0.325$	$\eta = 0.450$	$\eta = 0.650$
30	5	3.6	3.3	2.4	2.1	1.8	1.8	2
50	3.6	4.1	4.6	3.4	2.4	1.9	1.1	1.1
70	4.6	3.8	4.2	3.6	2.5	1.9	1.8	1.8
90	4.6	5	5	3.6	3.3	2.3	2.4	2.2

the characteristic points of the bottom plate of the stilling basin when $Q = 0.09\ m^3/s$.

By observing the power spectral density of the fluctuating pressure at the characteristic points in Figure 8, it can be found that the dominant frequency of fluctuating pressure in the front of the stilling basin with step-down floor is within 1.0 Hz, and the fluctuating energy is mainly concentrated in the frequency band of 0~10.0 Hz. The dominant frequency in the middle of the stilling basin with step-down floor is within 1~5.0 Hz, and the energy is concentrated in the low-frequency region; the dominant frequency of the stilling basin with step-down bottom is within 1.0 Hz, and

Table 5: Marginal spectral amplitude table ($\times 10^4$ Pa).

Q (m³/s)	$\eta = 0.025$	$\eta = 0.075$	$\eta = 0.125$	$\eta = 0.175$	$\eta = 0.225$	$\eta = 0.325$	$\eta = 0.450$	$\eta = 0.650$
30	9.2	10.3	5.9	2.7	2.3	2.1	1.8	8.4
50	168	419	78.5	35	37	26.8	23.6	7.4
70	340	1200	226	87	91.3	69.6	46	21.6
90	540	2040	430	144	133	113	88.6	46.5

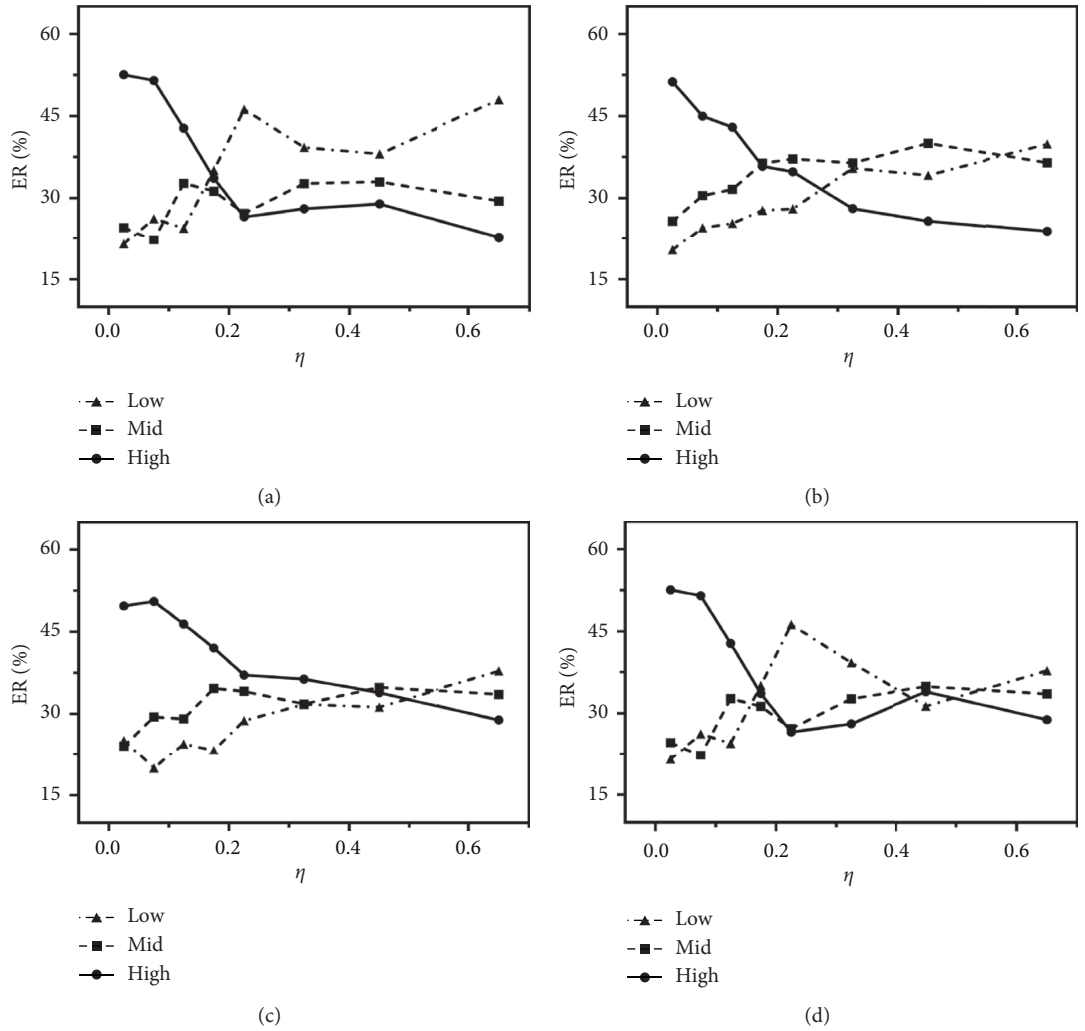

Figure 7: Proportions of energy in the high-, medium-, and low-frequency bands of each feature point: (a) $Q = 30$ m³/s; (b) $Q = 50$ m³/s; (c) $Q = 70$ m³/s; (d) $Q = 90$ m³/s.

the pulsating energy is mainly concentrated in the frequency band of 0~5.0 Hz. In the jet impingement region, the fluctuating pressure is controlled by large-scale vortex with large amplitude and low frequency, and its power spectrum is within 10.0 Hz. The dominant frequency of the jump head and the jump tail is more prominent, and the dominant frequency is distributed within 1.0 Hz. The proportion of high-frequency energy in the middle of the hydraulic jump increases, and the dominant frequency moves to high frequency.

By observing the Hilbert marginal spectrum of the feature points in Figure 8, it can be found that the dominant frequency of the stilling basin with step-down floor at the head and tail is very prominent, and most of the energy is concentrated below 1.0 Hz. The relative proportion of high-frequency energy in the middle segment of the stilling basin increases, and the dominant frequency moves to high frequency. This is consistent with the law obtained by Abdul Khader and Elango [25] and other scholars on the variation of pressure pulsation at the bottom of the hydraulic jump zone. Through comparative analysis, it is found that the FFT method and HHT method are consistent, which verifies that the HHT method is suitable for the analysis of fluctuating pressure signal of stilling basin with step-down floor.

From a probabilistic point of view, the Fourier spectrum can only reflect the probability that the frequency actually

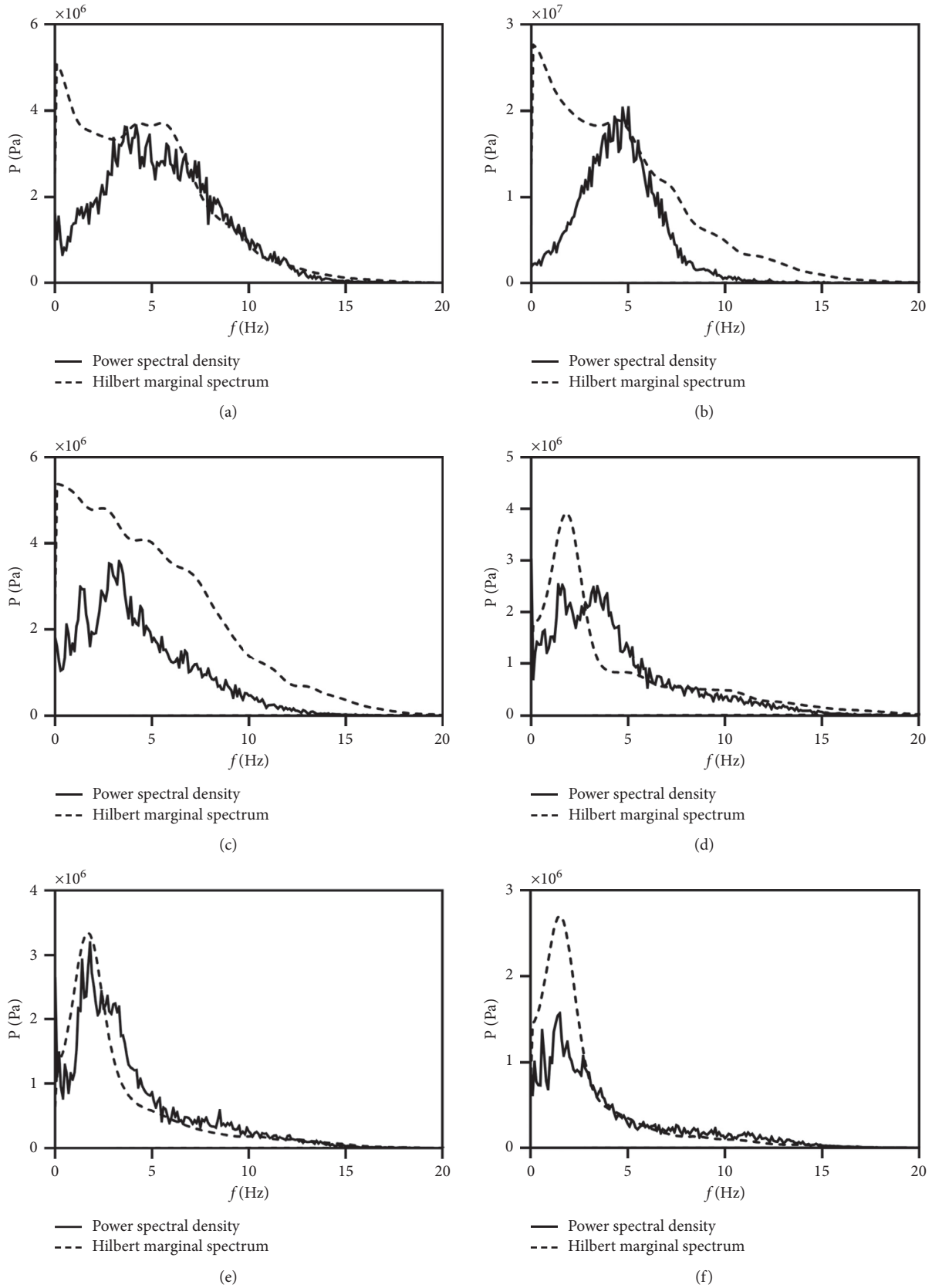

Figure 8: Continued.

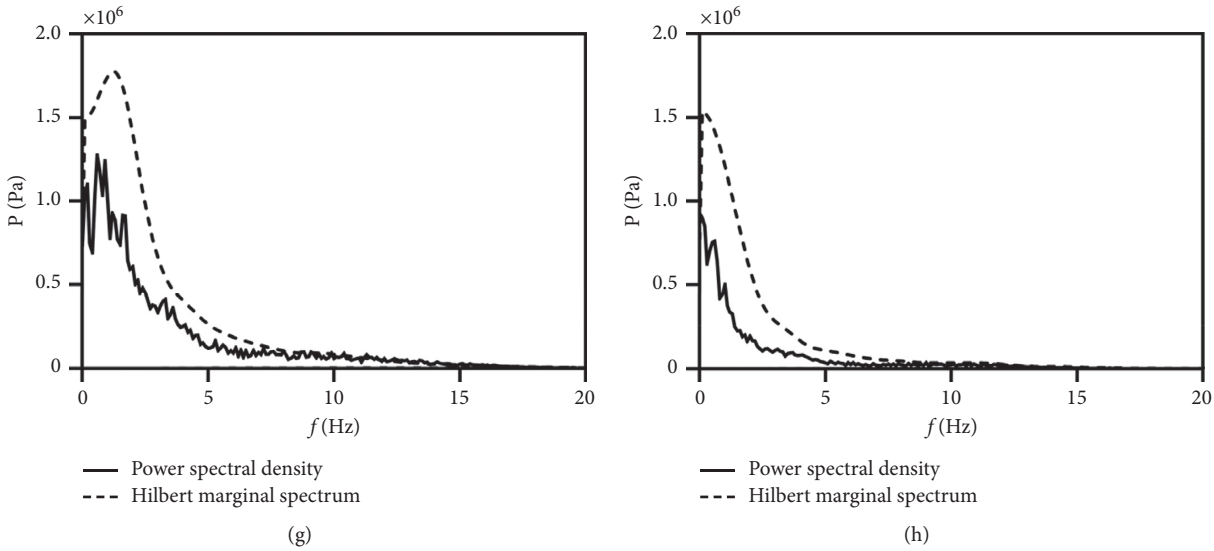

Figure 8: Hilbert marginal spectrum and power spectrum density diagram of characteristic points when $Q = 0.09\ m^3/s$: (a) $\eta = 0.025$; (b) $\eta = 0.075$; (c) $\eta = 0.125$; (d) $\eta = 0.175$; (e) $\eta = 0.225$; (f) $\eta = 0.325$; (g) $\eta = 0.45$; (h) $\eta = 0.65$.

exists in the signal, while the marginal spectrum can most truly reflect the characteristics of vibration, especially when analyzing nonstationary and nonlinear signals, the HHT method has more advantages. In the article "Feature Extraction of Ship Acoustic Signal Based on Hilbert–Huang Transform," Billy [26] mentioned that theoretically the frequency resolution of Hilbert's marginal spectrum is at least twice higher than that of Fourier theory, the advantage of the Hilbert marginal spectrum over Fourier amplitude spectrum, and its higher frequency resolution ability; Hwang et al. also concluded in "A note on analyzing nonlinear and nonstationary ocean wave data" that the resolution of the marginal spectrum of HHT is significantly higher than that of the Fourier power spectrum [27]. In this paper, when $Q = 90\ m^3/s$, the pulsating pressure signals of 8 characteristic points on the bottom of the stilling basin with step-down floor are processed by the HHT method and the FFT method, respectively. The results show that the resolution of the marginal spectrum obtained by the HHT method is higher, the local characteristics of the signal can be obtained more accurately, and the fluctuation characteristics of the marginal spectrum amplitude are more clearly reflected.

4. Conclusion

In this study, the HHT method was used to analyze the pulsating pressure signal, and the pulsating pressure signal on the stilling basin with step-down floor was studied from a different perspective from the traditional perspective, and the following conclusions were obtained:

(a) The pulsating pressure signal of the bottom of the stilling basin with step-down floor has obvious characteristics of low frequency and large amplitude; near the jet impact point, the signal energy is mainly concentrated in the low-frequency region; that is, the energy is mainly concentrated in the large-scale fluid vortex; the dominant frequency at the head and tail of the stilling basin is very prominent, and most of the energy is concentrated below 1.0 Hz. In the middle section of the stilling basin, the relative proportion of high-frequency energy increases, and the dominant frequency moves to high frequency; as the relative position of the measuring point increases, the energy distribution in the stilling basin with step-down floor changes from high-frequency component to low-frequency component, and the small-scale vortex in the stilling basin with step-down floor is transformed into large-scale vortex.

(b) The strong lateral movement of the water particle in the stilling basin with step-down floor causes the pulsating pressure signal to be a complex signal with interwave frequency modulation and intrawave frequency modulation. The Hilbert–Huang transform shows the nonlinear and nonstationary nature of the pressure pulsation and at the same time truly reveals that the pressure pulsation signal has nonlinear and random amplitude modulation and frequency modulation.

(c) Compared with the FFT method, the marginal spectrum obtained by the HHT method has higher resolution, more accurately obtains the local characteristics of the signal, and is more suitable for processing nonlinear and nonstationary signals.

Data Availability

The data used to support the findings of this study are available from the corresponding author upon reasonable request.

Conflicts of Interest

The authors declare there are no conflicts of interest with respect to the research, authorship, and/or publication of this article.

Acknowledgments

This thesis was completed under the guidance of Dr. Jiang Lei. The authors are grateful for his selfless help and support and wish him a smooth graduation and a bright future. This study was supported by the Sichuan Academic and Technical Leaders Training Fund (2012DTY020).

References

[1] J. Lian, X. Wang, W. Zhang, B. Ma, and D. Liu, "Multi-source generation mechanisms for low frequency noise induced by flood discharge and energy dissipation from a high dam with a ski-jump type spillway," *International Journal of Environmental Research and Public Health*, vol. 14, no. 12, p. 1482, 2017.

[2] F. Tajabadi, E. Jabbari, and H. Sarkardeh, "Effect of the end sill angle on the hydrodynamic parameters of a stilling basin," *The European Physical Journal Plus*, vol. 133, no. 1, p. 10, 2018.

[3] S. K. Sun, H. T. Liu, Q. F. Xia, and X. S. Wang, "Study on stilling basin with step-down floor for energy dissipation of hydraulic jump in high dams," *Journal of Hydraulic Engineering*, vol. 36, no. 10, pp. 1188–1193, 2005.

[4] D. Verschuren, "Sedimentation controls on the preservation and time resolution of climate-proxy records from shallow fluctuating lakes," *Quaternary Science Reviews*, vol. 18, no. 6, pp. 821–837, 1999.

[5] V. N. Zhivoderov and N. I. Tupikov, "Effective fastening of the bottom of the stilling basin of a high-head dam by prestressed anchors," *Hydrotechnical Construction*, vol. 28, no. 4, pp. 243–252, 1994.

[6] Y. Lu, J. Yin, Z. Yang, K. Wei, and Z. Liu, "Numerical study of fluctuating pressure on stilling basin slab with sudden lateral enlargement and bottom drop," *Water*, vol. 13, no. 2, p. 238, 2021.

[7] V. Armenio, P. Toscano, and V. Fiorotto, "On the effects of a negative step in pressure fluctuations at the bottom of a hydraulic jump," *Journal of Hydraulic Research*, vol. 38, no. 5, pp. 359–368, 2000.

[8] F. Kazemi, S. R. Khodashenas, and H. Sarkardeh, "Experimental study of pressure fluctuation in stilling basins," *International Journal of Civil Engineering*, vol. 14, no. 1, pp. 13–21, 2016.

[9] M. Yang, H. P. Li, and W. J. Feng, "Experimental study on fluctuating pressure of stilling basin with drop sill," *Progress in Water Conservancy and Hydropower Science and Technology*, vol. 91, no. 2, pp. 24–29, 2016.

[10] N. E. Huang, M. L. Wu, W. Qu, S. R. Long, and S. Shen, "Applications of Hilbert-Huang transform to non-stationary financial time series analysis," *Applied Stochastic Models in Business and Industry*, vol. 19, no. 3, pp. 245–268, 2010.

[11] Y. Q. Zhang, Y. T. Zhu, Y. Zheng, Y. Feng, X. F. Ge, and X. Q. Tian, "Research on the fault characteristic extraction of hydropower units based on hilbert-huang transform," *Applied Mechanics and Materials*, vol. 607, pp. 633–637, 2014.

[12] X. Jing and Q. Li, "A nonlinear decomposition and regulation method for nonlinearity characterization," *Nonlinear Dynamics*, vol. 83, no. 3, pp. 1–23, 2016.

[13] S. K. Jain and S. N. Singh, "Harmonics estimation in emerging power system: key issues and challenges," *Electric Power Systems Research*, vol. 81, no. 9, pp. 1754–1766, 2011.

[14] F. Kai, J. Qu, C. Yi, and D. Yong, "Classification of seizure based on the time-frequency image of EEG signals using HHT and SVM," *Biomedical Signal Processing and Control*, vol. 13, pp. 15–22, 2014.

[15] R. Kumar, B. Singh, and D. T. Shahani, "Recognition of single-stage and multiple power quality events using hilbert-huang transform and probabilistic neural network," *Electric Power Components and Systems*, vol. 43, no. 6, pp. 607–619, 2015.

[16] C. K. Hemapriya, M. V. Suganyadevi, and C. Krishnakumar, "Detection and classification of multi-complex power quality events in a smart grid using Hilbert–Huang transform and support vector machine," *Electrical Engineering*, vol. 102, no. 4, 2020.

[17] N. E. Huang, M.-L. Wu, W. Qu, S. R. Long, and S. S. P. Shen, "Applications of Hilbert-Huang transform to non-stationary financial time series analysis," *Applied Stochastic Models in Business and Industry*, vol. 19, no. 3, pp. 245–268, 2003.

[18] Z. Peng, W. T. Peter, and F. Chu, "An improved Hilbert–Huang transform and its application in vibration signal analysis," *Journal of Sound Vibration*, vol. 286, no. 1-2, pp. 187–205, 2005.

[19] H. Ding, Z. Huang, Z. Song, and Y. Yan, "Hilbert-Huang transform based signal analysis for the characterization of gas-liquid two-phase flow," *Flow Measurement and Instrumentation*, vol. 18, no. 1, pp. 37–46, 2007.

[20] N. E. Huang, Z. Shen, S. R. Long et al., "The empirical mode decomposition and the Hilbert spectrum for nonlinear and non-stationary time series analysis," *Proceedings of the Royal Society of London. Series A: Mathematical, Physical and Engineering Sciences*, vol. 454, no. 1971, pp. 903–995, 1998.

[21] C. Pappone, S. Rosanio, D. Burkhoff et al., "Cardiac contractility modulation by electric currents applied during the refractory period in patients with heart failure secondary to ischemic or idiopathic dilated cardiomyopathy," *The American Journal of Cardiology*, vol. 90, no. 12, pp. 1307–1313, 2002.

[22] V. Yakhot and S. A. Orszag, "Renormalization group analysis of turbulence. I. basic theory," *Journal of Scientific Computing*, vol. 1, no. 1, pp. 3–51, 1986.

[23] C. von Randow, B. Kruijt, and A. A. Holtslag, "Low-frequency modulation of the atmospheric surface layer over Amazonian rain forest and its implication for similarity relationships," *Agricultural Forest Meteorology*, vol. 141, no. 2-4, pp. 192–207, 2006.

[24] J. Cheng, D. Yu, J. Tang, and Y. Yang, "Application of frequency family separation method based upon EMD and local Hilbert energy spectrum method to gear fault diagnosis," *Mechanism and Machine Theory*, vol. 43, no. 6, pp. 712–723, 2008.

[25] M. H. Abdul Khader and K. Elango, "Turbulent pressure field beneath a hydraulic jump," *Journal of Hydraulic Research*, vol. 12, no. 4, pp. 469–489, 1974.

[26] M. de Billy, "Determination of the resonance spectrum of elastic bodies via the use of short pulses and Fourier transform theory," *Journal of the Acoustical Society of America*, vol. 79, no. 2, pp. 219–221, 1986.

[27] P. A. Hwang, N. E. Huang, and D. W. Wang, "A note on analyzing nonlinear and nonstationary ocean wave data," *Applied Ocean Research*, vol. 25, no. 4, pp. 187–193, 2003.